Nano Research
DOI 10.1007/s12274-014-0475-2
Research Article
ISSN 1998-0124
CN 11-5974/O4

$SnO_2@Co_3O_4$ Hollow Nano-spheres for a Li-ion Battery Anode with Extraordinary Performance

Won-Sik Kim, Yoon Hwa, Hong-Chan Kim, Jong-Hyun Choi, Hun-Joon Sohn, and Seong-Hyeon Hong(✉)

Nano Res., **Just Accepted Manuscript** • DOI: 10.1007/s12274-014-0475-2
http://www.thenanoresearch.com on April 10, 2014

Just Accepted

TSINGHUA UNIVERSITY PRESS Springer

$SnO_2@Co_3O_4$ Hollow Nano-spheres for a Li-ion Battery Anode with Extraordinary Performance

This template is to be used for preparing manuscripts for submission to *Nano Research*. Use of this template will save time in the review and production processes and will expedite publication. However, use of the template is not a requirement of submission. Do not modify the template in any way (delete spaces, modify font size/line height, etc.). If you need more detailed information about the preparation and submission of a manuscript to Nano Research, please see the latest version of the Instructions for Authors at http://www.thenanoresearch.com/.

TABLE OF CONTENTS (TOC)

$SnO_2@Co_3O_4$ Hollow Nano-spheres for a Li-ion Battery Anode with Extraordinary Performance

Won-Sik Kim, Yoon Hwa, Hong-Chan Kim, Jong-Hyun Choi, Hun-Joon Sohn, and Seong-Hyeon Hong*

Department of Materials Science and Engineering and Research Institute of Advanced Materials, Seoul National University, Republic of Korea

Page Numbers. The font is ArialMT 16 (automatically inserted by the publisher)

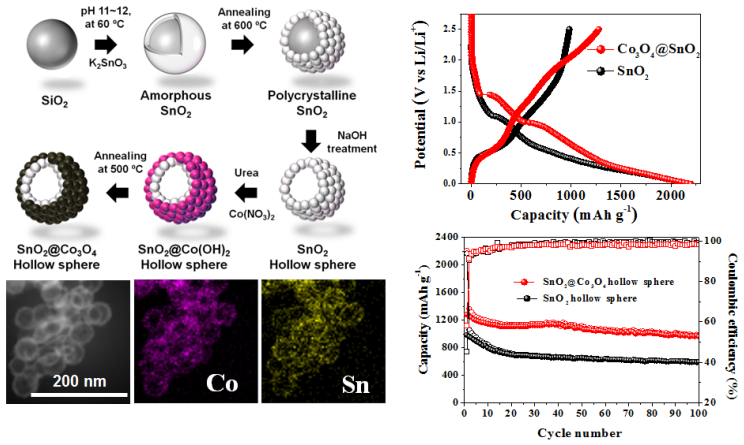

Facile route for the synthesis of $SnO_2@Co_3O_4$ hollow spheres and extraordinary performance as an anode for lithium-ion battery.

Nano Res
DOI (automatically inserted by the publisher)
Research Article Please choose one

$SnO_2@Co_3O_4$ Hollow Nano-spheres for a Li-ion Battery Anode with Extraordinary Performance

Won-Sik Kim, Yoon Hwa, Hong-Chan Kim, Jong-Hyun Choi, Hun-Joon Sohn, and Seong-Hyeon Hong(✉)

Department of Materials Science and Engineering and Research Institute of Advanced Materials, Seoul National University, Seoul 151-744, Republic of Korea.

Received: day month year / Revised: day month year / Accepted: day month year (automatically inserted by the publisher)

ABSTRACT

$SnO_2@Co_3O_4$ hollow nano-spheres were prepared using the template-based sol-gel coating technique and their electrochemical performance as an anode for lithium ion battery (LIB) was investigated. The size of synthesized hollow spheres was about 50 nm with the shell thickness of 7~8 nm. The fabricated $SnO_2@Co_3O_4$ hollow nano-sphere electrode exhibited an extraordinary reversible capacity (962 mAh g^{-1} after 100 cycles at 100 mA g^{-1}), good cyclability, and high rate capability, which was attributed to the Co enhanced reversibility of the Li_2O reduction reaction during cycling.

KEYWORDS

Hollow sphere, lithium ion battery, anode, SnO_2, Co_3O_4

1. Introduction

Carbon-based materials are commonly used as an anode for lithium-ion batteries (LIBs), but low theoretical capacity (372 mAh g^{-1}) and safety are the major concern for large-scale storage applications [1, 2]. The intensive researches have focused on high capacity electrode materials such as Si, Ge, and Sn [3-5]. Among various candidates, SnO_2 is one of the promising anode materials due to its high capacity and low reactivity with electrolyte [6, 7]. However, a severe volume change occurs during lithium insertion/extraction, which causes a pulverization and electrical connectivity loss. The aggregation of small and active Sn particles into larger and inactive Sn clusters during cycling also contributes to a fast capacity fading [8]. Nanostructured SnO_2 such as nano-particles, nano-tubes, nano-wires, nano-hollow spheres, and meso-porous structure is considered as an effective approach to improve the cycling performance [8-14]. Among them, hollow nano-spheres are the most promising structure for the anode electrode of LIBs, but in most of the previous studies, the size of hollow spheres was limited to 100-200 nm and the capacity fading was still observed [13,15,16]. In our previous study, it was

Address correspondence to Seong-Hyeon Hong, email; shhong@snu.ac.kr

demonstrated that nano-sized SnO_2 hollow spheres with ~5 nm shell thickness exhibited the high reversible capacity and excellent cyclability without the capacity fading, and the aggregation of Sn was not observed [17].

Recently, nano-sized transition-metal oxides (MO, where M is Co, Ni, Cu, or Fe) are known to reversibly react with Li ions, and they become a new type of anode material for LIBs [16]. Among them, cobalt oxide (CoO or Co_3O_4) is a promising anode material due to its high theoretical capacity and catalytic behavior [18-21]. However, poor electrical conductivity and structural instability are the drawback of cobalt oxide as an anode for LIBs [19]. To enhance the lithium storage performance, hybridization of nano-structured cobalt oxide with other materials is actively explored, and SnO_2 is one of the representative hybridizing materials [22-27]. The SnO_2/cobalt oxide composite electrodes exhibit the synergistic effect in initial few cycles, but in most of cases, the reversible capacity slowly decreased [28,29]. The structural instability of core material and detachment of shell layer during repeated cycling appear to be the main reasons for the capacity fading.

Herein, we fabricate the SnO_2@Co_3O_4 double-shell hollow nano-sphere electrode using the template-based sol-gel coating technique, and demonstrate the excellent electrochemical performance of the composite electrode as an anode for LIBs. Our strategy of the structural design is as follows. The nano-sized hollow SnO_2 sphere can accommodate the large volume change without a pulverization of electrical pathways and provide the short diffusion path of Li^+ within the thin shell layer, which lead to the excellent cyclability and rate capability [17]. Thus, we employed the 50 nm-sized SnO_2 hollow nano-spheres with the shell thickness of 5 nm as a core material. For the synergistic effects, Co_3O_4 shell was coated on the core SnO_2 and the shell thickness was limited to 2~3 nm to avoid the detachment or pulverization. The Co nanoparticles decomposed from the Co_3O_4 shell during lithiation can increase the reversibility of the reduction reaction of Li_2O formed during the discharge of SnO_2 and contribute to the extra reversible capacity [21]. Indeed, the fabricated SnO_2@Co_3O_4 hollow nano-sphere electrode shows an impressive electrochemical performance with an extraordinary reversible capacity (962 mAh g^{-1} after 100 cycles at 100 mA g^{-1}), good cyclability, and high rate capability. Furthermore, we examined the charging/discharging reactions of SnO_2@Co_3O_4 hybrid electrode using ex-situ TEM and confirmed the suggested synergistic effects.

2. Experimental

2.1 Synthesis of SnO_2 hollow spheres

The SnO_2 hollow sphere was prepared by using SiO_2 colloid solution [17]. 0.5 g of potassium stannate trihydrate ($K_2SnO_3 \cdot 3H_2O$, Sigma Aldrich,) was dissolved into 45 mL deionized water and 5 mL of prepared SiO_2 colloid solution was added. And then, 25 mL of absolute ethanol was added into above solution. The solution was heated to 60 °C for 1 h with a mild stirring. The white product was collected by centrifuge and washed with deionized water three times, dried at 100 °C, and annealed at 600 °C for 1 h. The annealed powder was treated with 2 M NaOH solution at 50 °C for 1 h. After that, the SnO_2 hollow sphere was obtained.

2.2 Co_3O_4 coating on SnO_2 hollow spheres

0.1 g of SnO_2 hollow sphere was dispersed in D. I. water and 0.18 g $Co(NO_3)_2 \cdot 6H_2O$, 1 g of PVP (Polyvinylpyrrolidone), and 2.4 g of urea ($CO(NH_2)_2$) were added. And then, the solution was heated at 80 °C for 10 h with mild stirring. The obtained power was washed by D. I. water, dried, and heated at 500 °C for 1 h.

2.3 Electrochemical test

For electrochemical measurements, the test electrodes consisted of active powder material (0.2 g), carbon black (Ketchen Black, 0.06 g) as a conducting agent and poly amide imide (PAI, 0.029 g) dissolved in N-methyl pyrrolidinone (NMP) at 60 °C as a binder. Each component was well mixed to form a slurry using a magnetic stirrer. The slurry was coated on a copper foil substrate, pressed, and dried at 200 °C for 4 h under a vacuum. A coin-type electrochemical cell was used with Li foil as the

counter and reference electrodes, and 1 M $LiPF_6$ in ethylene carbonate (EC)/diethylene carbonate (DEC) (5:5 (v/v), PANAX) was used as the electrolyte. The cell assembly and all electrochemical tests were carried out in an Ar-filled glove box. The cycling experiments were galvanostatically performed using a Maccor automated tester at a constant current density of 100 mA g^{-1} for the active material within a voltage range between 0.0 and 2.5 V (vs. Li/Li^+).

3. Results and discussion

The fabrication procedure for SnO_2@Co_3O_4 hollow nano-spheres is schematically shown in Fig. 1(a). For the template-based synthesis of nano-sized SnO_2 hollow spheres, SiO_2 colloid solution was prepared by a modified stöbber method [30]. Amorphous SnO_2 was coated on SiO_2 template by a sol-gel method using potassium stannate trihydrate [31]. After centrifuging and washing with deionized water, SiO_2@SnO_2 spheres were annealed at 600 °C for SnO_2 crystallization. The SnO_2 hollow spheres were obtained by removing the SiO_2 cores in 2M NaOH solution. The SnO_2@Co_3O_4 hollow nano-spheres were achieved by coating the $Co(OH)_2$ shell on the SnO_2 hollow spheres using cobalt (II) nitrate hexahydrate, polyvinylpyrrolidone, and urea and annealing at 500 °C. Urea was used for a slow hydrolysis of $Co(OH)_2$, which lead to a heterogeneous nucleation (coating) [32-36]. The SnO_2 hollow spheres had a quite uniform diameter and their surface became slightly rough after $Co(OH)_2$ coating and annealing at 500 °C (Fig. 1(b) and (c), Fig. S-1 in the ESM). The size of hollow spheres was not significantly changed during coating and annealing processes.

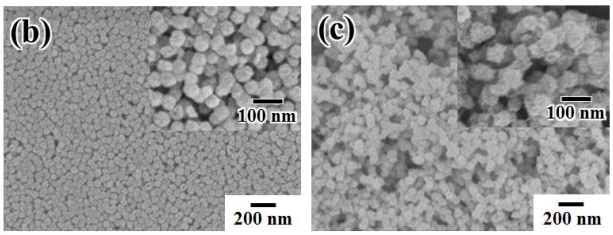

Figure 1 (a) Schematic illustration of synthesis procedure for SnO_2@Co_3O_4 hollow nano-spheres, (b) and (c) SEM images of SnO_2 and SnO_2@Co_3O_4 hollow spheres.

The fabricated SnO_2@Co_3O_4 hollow spheres were characterized by transmission electron microscopy (TEM). The low magnification TEM image revealed the hollow structure with bright-colored center (cavity) and dark-colored shell (SnO_2@Co_3O_4 layer) (Fig. 2(a)). The hollow spheres had the relatively uniform diameter (~50 nm). The individual hollow spheres were more or less agglomerated. The selected area electron diffraction (SAED) pattern exhibited the ring pattern, which was indexed to be a rutile SnO_2 (inset of Fig. 2(a)), and the diffraction peaks related to the cobalt oxide were not detected. The high magnification TEM image shows that the shell of hollow spheres was composed of interconnected nanocrystallites of 2~3 nm size (Fig. 2(b)). The shell thickness was estimated to be 7~8 nm, which was thicker than that of SnO_2 hollow spheres (~5 nm) (Fig. S-1 in the ESM). However, the outer Co_3O_4 layer could not be distinguished from the inner SnO_2 layer. The scanning transmission electron microscopy (STEM) image and energy dispersive x-ray spectroscopy (EDS) mappings indicate that Sn and Co were uniformly distributed over the entire surface of the hollow spheres (Fig. 2(c)~(e)). Two signals were overlapped and could not be separated each other (Fig. S-2 in the ESM). The atomic ratio of Co to Sn determined by EDS was ~0.46 (Fig. S-3 in the ESM), and it can be said that cobalt oxide was coated on tin oxide yielding the double shell hollow nano-spheres. To determine the specific surface area, Brunauer-Emmett-Teller (BET) nitrogen absorption /desorption analysis was performed. The BET surface area of SnO_2 and SnO_2@Co_3O_4 hollow spheres was 84.32 and 84.47 $m^2\ g^{-1}$, respectively (Fig. S-4 in the ESM). Thus, the surface area remained constant irrespective of Co_3O_4 coating. The crystal structure of the hollow spheres was further investigated by X-ray

diffraction (XRD) (Fig. 2(f)). All the diffraction peaks were broadened due to the nano-crystalline nature of the hollow spheres, but they were indexed to be a rutile SnO_2 (ICDD # 41-1445). After coating of $Co(OH)_2$ on SnO_2, the peaks for $Co(OH)_2$ were not detected by XRD and FT-IR. To reveal the phase of as-coated layer, we prepared the $Co(OH)_2$ powder without SnO_2 core in the same experimental conditions. The XRD pattern indicates that coating layer was α-$Co(OH)_2$ (Fig. S-5 in the ESM) [37]. From this result, we speculate that α-$Co(OH)_2$ was formed on the surface of SnO_2 hollow sphere during coating. In $SnO_2@Co_3O_4$ hollow spheres, the diffraction peaks for cobalt oxide could not be resolved, either, and the intensity was slightly reduced compared to that of SnO_2 hollow spheres, which implies that the coated cobalt oxide might be non-crystalline. The chemical states of Co and Sn in the hollow spheres were investigated using XPS, and the core level Co2p spectrum is shown in Fig. 2(g). The spectrum exhibited two peaks at 780.5 ($Co2p_{3/2}$) and 796.2 ($Co2p_{1/2}$) eV. The observed binding energy of Co was in good agreement with the value for Co_3O_4 [38, 39]. All the hollow spheres showed a Sn3d doublet with a $Sn3d_{5/2}$ at 486.43~486.52 eV (inset of Fig. 2g), which corresponds to SnO_2 [40]. Thus, $SnO_2@Co_3O_4$ double shell hollow nano-spheres were successfully synthesized and the outer cobalt oxide shell appeared to be amorphous Co_3O_4.

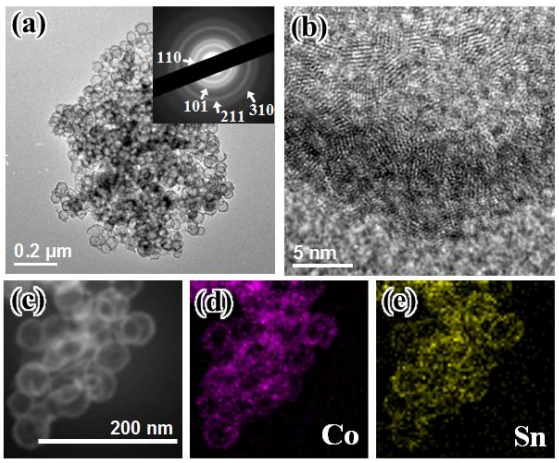

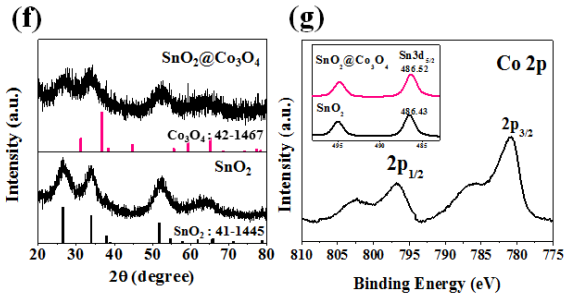

Figure 2 (a) and (b) TEM images of $SnO_2@Co_3O_4$ hollow spheres, (c) STEM image of $SnO_2@Co_3O_4$ hollow spheres, (d) Co and (e) Sn EDS mapping of (c), (f) XRD patterns of hollow spheres, and (g) Co2p XPS spectrum of $SnO_2@Co_3O_4$ hollow spheres.

The electrochemical cell tests of SnO_2 and $SnO_2@Co_3O_4$ hollow nano-sphere electrodes were galvanostatically conducted, and the discharge /charge voltage profiles are shown in Fig. 3(a) and (b), respectively. The discharge and charge capacities of SnO_2 hollow nano-sphere electrode were 2167 and 981 mAh g^{-1}, respectively, with an initial Coulombic efficiency of ~45 % (Fig. 3(a)). The irreversible capacity loss is attributed to the formation of irreversible Li_2O and solid electrolyte interphase (SEI) on the surface of active material [6]. On the other hands, the discharge and charge capacities of $SnO_2@Co_3O_4$ hollow nano-sphere electrode were 2208 and 1280 mAh g^{-1}, respectively, with an initial Coulombic efficiency of ~58 % (Fig. 3(b)). Thus, $SnO_2@Co_3O_4$ electrode exhibited higher initial discharge and charge capacities and Coulombic efficiency than those of SnO_2 electrode. In addition, the first discharge voltage profile of $SnO_2@Co_3O_4$ electrode exhibited an additional voltage plateau at 1.4 V, which implies that Co_3O_4 reacts with Li. The fabrication of Co_3O_4 hollow nano-sphere was not successful in this study because the hollow spheres were collapsed during SnO_2 etching process. However, it was reported that needle-like Co_3O_4 nanotubes had the reversible capacity of 918 mAh g^{-1} after 30 cycles at the current density of 50 mA g^{-1} [19]. The cyclabilities of SnO_2 and $SnO_2@Co_3O_4$ hollow nano-sphere electrodes were compared at a current density of 100 mA g^{-1} (Fig. 3(c)). After 100 cycles, the reversible discharge and charge capacities of SnO_2 electrode were 601 and 592 mAh g^{-1}, respectively, with a cycle retention of 27 % (based on the discharge capacity of the first cycle) whereas the

discharge and charge capacities of $SnO_2@Co_3O_4$ electrode were 982 and 962 mAh g^{-1}, respectively, with the cycle retention of 44 %. For $SnO_2@Co_3O_4$ electrode, the reversible capacity maintained 721 mAh g^{-1} even at a higher current density of 500 mA g^{-1} after 50 cycles (Fig. S-6 in the ESM). Thus, $SnO_2@Co_3O_4$ electrode showed a much stable cycling performance. The observed reversible capacity of 962 mAh g^{-1} for $SnO_2@Co_3O_4$ electrode was higher than the theoretical capacity of either SnO_2 (781 mAh g^{-1}) or Co_3O_4 (890 mAh g^{-1}) electrode. This synergistic behavior is understood as follows. The Co nanoparticle is known to enhance the reversibility of Li_2O reduction reaction [21], which implies that Li_2O, formed during the discharge of SnO_2, is more active by introducing the outer Co_3O_4 shell. As a result, the recombination of Li_2O and Sn is accelerated. Recently, it was reported that Li_2O and Sn partially recombine to form SnO or SnO_2 [41-44]. In that case, the theoretical capacity of SnO_2 electrode is 1494 mAh g^{-1}. Therefore, a large reversible capacity of $SnO_2@Co_3O_4$ hollow nano-sphere electrode up to 962 mAh g^{-1} is possible if Li_2O is partially reversible during cycling. In addition, a reversible growth of gel-like polymeric layer on the surface of Co_3O_4 can contribute to the extra reversible capacity [20]. The capacity contributions from each component or reaction have been estimated and the detailed calculations are in ESM. The rate capability of SnO_2 and $SnO_2@Co_3O_4$ hollow nano-sphere electrodes is illustrated in Fig. 3(d) and (e). Both electrodes showed a good rate capability, but $SnO_2@Co_3O_4$ electrode exhibited the higher reversible capacities at all current densities. At the current density of 500 mA g^{-1}, the reversible capacities of SnO_2 and $SnO_2@Co_3O_4$ electrodes were 590 and 850 mAh g^{-1}, respectively. In particular, $SnO_2@Co_3O_4$ electrode still showed the high reversible capacity of 750 mAh g^{-1} at a higher current density of 900 mA g^{-1}. This good rate capability is attributed to the short diffusion path of Li ion within Co_3O_4 outer and SnO_2 inner shells. We have tried to change the thickness of Co_3O_4 shell by increasing the amount of Co precursor, but a severe aggregation occurred and Co_3O_4 nano-platelets were formed in high Co precursor content (Fig. S-7 in the ESM). Furthermore, this electrode showed a relatively fast capacity fading. Recently, Co_3O_4-SnO_2 core-shell nanorods (or nanoneedles) have been fabricated and the synergistic effects have been observed in these nanostructures, but they still showed a capacity fading [28, 29]. Thus, we concluded that hollow SnO_2 core with thin Co_3O_4 shell can effectively alleviate the volume expansion/contraction during cycling resulting in the increased specific capacity and improved cycling performance.

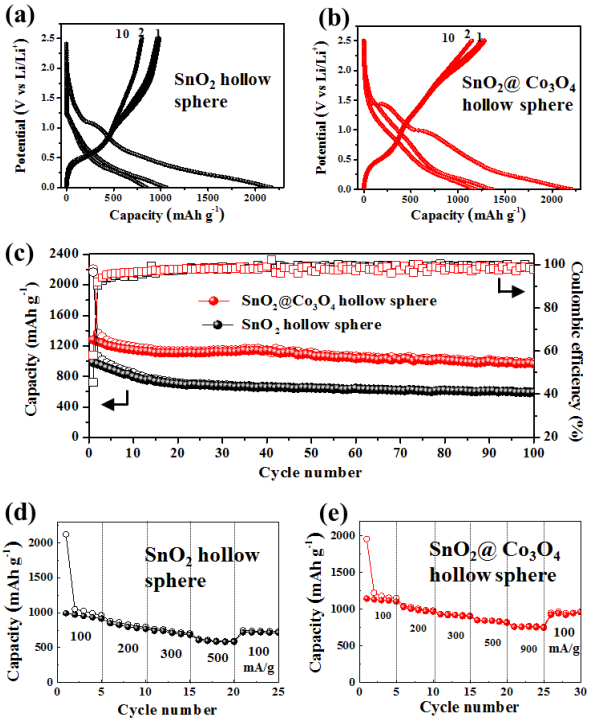

Figure 3 (a) and (b) Voltage profiles of SnO_2 and $SnO_2@Co_3O_4$ hollow spheres between 0.01 and 2.5 V at 100 mA g^{-1}, (c) cycling performance of SnO_2 and $SnO_2@Co_3O_4$ hollow spheres at 100 mA g^{-1}, and (d) and (e) rate capability test of SnO_2 and $SnO_2@Co_3O_4$ hollow spheres, respectively.

To identify the Li-ion charge/discharge reactions in the $SnO_2@Co_3O4$ electrode, ex-situ TEM analysis was carried out at the selected potentials marked in the differential capacity plot (DCP), and the corresponding TEM images and SAED patterns for the active anode materials are illustrated in Fig. 4. In the first cycle of the DCP (Fig. 4(a)), there were three reduction peaks at 1.44, 0.99, and 0.20 V. The reduction peak at 1.44 V is ascribed to the formation of $Li_xCo_3O_4$ phase [20, 21, 45], and 0.99 and 0.20 V peaks are attributed to the reduction of $Li_xCo_3O_4$ to Co according to $Li_xCo_3O_4 + (8\text{-}x)Li + +(8\text{-}x)e^- \rightarrow 3Co + 4Li_2O$ and the reduction of SnO_2 to Sn according to $SnO_2 + 4Li^+ + 4e^- \rightarrow Sn + 2L_2O$ [6, 45], respectively. With these reactions, the formation of solid electrolyte interface (SEI) layer simultaneously

occurs. In the oxidation half cycle, two oxidation peaks at 0.49 and 1.2 V correspond to the delithiation of Li_xSn alloy into Sn and the decomposition of Li_2O, respectively. And the third oxidation peak of 2.0 V is ascribed to the oxidation reaction to Co_3O_4 and SnO_x [43-46]. Ex-situ XRD analysis was also conducted, but no diffraction peak was observed except the peaks for Cu substrate (Fig. S-8 in the ESM). When the potential was lowered to 1.20 V (Fig. 4(b)), unreacted SnO_2 and $Li_xCo_3O_4$ (ICDD #39-0846), which is the intermediate phase of lithiated Co_3O_4, were observed [19, 45]. At 0.68 V (Fig. 4(c)), Sn (ICDD #18-1380) and Co (ICDD #15-0806), which were decomposed from SnO_2 and Co_3O_4, respectively, were detected, while Li_2O was not identified due to the amorphous nature. When the potential reached 0.0 V (Fig. 4(d)), $Li_{22}Sn_5$ (ICDD #18-0753) was observed, which agrees with the previous report on Sn electrode [6]. As seen in Fig. 4(d), the hollow structure was well maintained despite a large volume expansion with a full-lithiation. During the charging process, $Li_{22}Sn_5$ phase was decomposed to Sn, as observed at 0.90 V (Fig. 4(e)). When the electrode was fully delithiated to 2.50 V, the hollow structure was still maintained, and metallic Sn, SnO (ICDD #06-0395), and Co_3O_4 phases were identified. Thus, the partial recombination reaction between Sn and Li_2O to form SnO was confirmed.

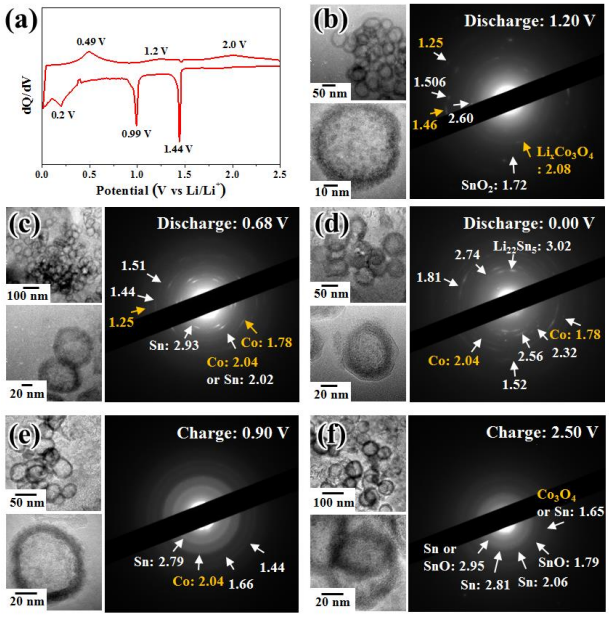

Figure 4 (a) DCP (differential capacity plot) of $SnO_2@Co_3O_4$ hollow sphere electrode during the first cycle. Ex-situ TEM analyses of $SnO_2@Co_3O_4$ hollow sphere electrode, lithiation process: (b) 1.20 V, (c) 0.68 V, and (d) 0.00 V; delithiation process: (e) 0.90 V and (f) 2.50 V.

Based on ex-situ TEM analysis, the following reaction mechanism is suggested for $SnO_2@Co_3O_4$ hollow nano-sphere electrode:

During lithiation:

$$5SnO_2 + Co_3O_4 + 50Li^+ + 50e^- \rightarrow Li_{22}Sn_5 + 3Co + 14Li_2O \quad (1)$$

During delithiation:

$$Li_{22}Sn_5 + 3Co + 14Li_2O \rightarrow (5-x)Sn + xSnO + (3-3y)Co + yCo_3O_4 + (14-x-4y)Li_2O + (2x+8y)Li^+ + (2x+8y)e^- \quad (2)$$

Here, x ($0 \le x \le 1$) and y ($0 \le y \le 1$) are the fractional amount of recombined SnO and Co_3O_4, respectively.

The ex-situ TEM images also demonstrated the structural stability of $SnO_2@Co_3O_4$ hollow nanosphere electrode during the cycling test. The hollow cavity well accommodated the large volume change, and the structural deformation or severe aggregation was not observed after 100 cycles (Fig. 5).

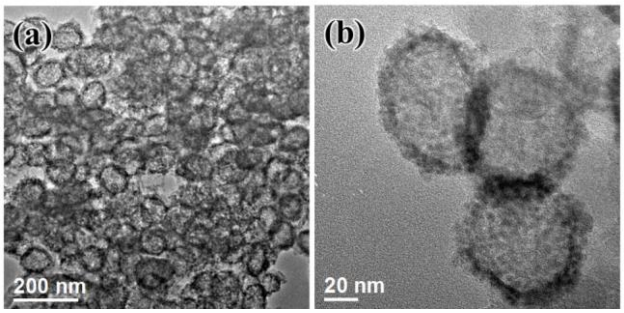

Figure 5 TEM images of $SnO_2@Co_3O_4$ hollow spheres after 100 cycles at 100 mA g^{-1}.

4. Concluisons

$SnO_2@Co_3O_4$ hollow nano-spheres were successfully synthesized by using SiO_2 nano-colloid as sacrificial template. The size of synthesized hollow spheres was ~50 nm with the shell thickness of 7~8 nm. By introducing the outer Co_3O_4 shell to SnO_2 hollow sphere, the reversible capacity increased from 592 to 962 mAh g^{-1} after 100 cycles at a current density of 100 mA g^{-1}. The large reversible capacity of $SnO_2@Co_3O_4$ hollow nano-sphere electrode was

attributed to the Co enhanced reversibility of the Li_2O reduction reaction during cycling. The high reversible capacity and cycle stability of SnO_2@Co_3O_4 composite suggests that it is a promising anode for the next-generation LIBs, and the design strategy of this work can be applied to other metal oxides-SnO_2 composites as well as other applications.

Acknowledgements

This work was supported by the National Research Foundation of Korea (NRF) grant funded by the Korea Government (MSIP) (NRF-2012R1A2A 4A0100 8226).

Electronic Supplementary Material: Supplementary material (TEM and EDS analysis, nitrogen absorption/desorption isotherm, and pore size distribution plot, and electrochemical test) is available in the online version of this article at http://dx.doi.org/10.1007/s12274-***-****-*.

References

[1] Endo, M.; Kim, C.; Nishimura, K.; Fujino, T.; Miyashita, K. Recent development of carbon materials for Li ion batteries. *Carbon*, **2000**, 38, 183-197.

[2] Winter, M.; Besenhard, J. O.; Spahr, M. E.; Novák, P. Insertion electrode materials for rechargeable lithium batteries. *Adv. Mater*. **1998**, 10, 725-763.

[3] Boukamp, B. A.; Lesh, G. C.; Huggins, R. A. All–solid lithium electrodes with mixed–conductor matrix. *J. Electrochem. Soc*. **1981**, 128, 725-729.

[4] Winter, M.; Besenhard, J. O. Electrochemical lithiation of tin and tin-based intermetallics and composites. *Electrochimica Acta*, **1999**, 45, 31-50.

[5] Chang, W.–S.; Park, C.–M.; Kim, J.–H.; Kim, Y.–U.; Jeong, G.; Sohn, H.–J. Quartz (SiO_2): a new energy storage anode material for Li-ion batteries. *Energy Environ. Sci*. **2012**, 5, 6895-6899.

[6] Courtney, I. A.; Dahn, J. R. Electrochemical and in situ X-ray diffraction studies of the reaction of lithium with tin oxide composites. *J. Electrochem. Soc*. 1997, 144, 2045-2052.

[7] Chen, J. S.; Lou, X. W. SnO_2-based nanomaterials: synthesis and application in lithium-ion batteries. *Small*, **2013**, 9, 1877-1893.

[8] Kim, C.; Noh, M.; Choi, M.; Cho, J.; Park, B. Critical size of a nano SnO_2 electrode for Li-secondary battery. *Chem. Mater*. **2005**, 17, 3297-3301.

[9] Ye, J.; Zhang, H.; Yang, R.; Li, X.; Qi, L. Morphology-controlled synthesis of SnO_2 nanotubes by using 1D silica mesostructures as sacrificial templates and their applications in lithium-ion batteries. *Small*, **2010**, 6, 296-306.

[10] Kim, W.–S.; Lee, B.–S.; Kim, D.–H.; Kim, H.–C.; Yu, W.–R.; Hong, S.–H. SnO_2 nanotubes fabricated using electrospinning and atomic layer deposition and their gas sensing performance. *Nanotechnology*, **2010**, 21, 245605.

[11] Chan, C. K.; Peng, H.; Liu, G.; McIlwrath, K.; Zhang, X. F.; Huggins, R. A.; Cui, Y. High-performance lithium battery anodes using silicon nanowires. *Nature Nanotechnology*, **2008**, 3, 31-35.

[12] Huang, J. Y.; Zhong, L.; Wang, C. M.; Sullivan, J. P.; Xu, W.; Zhang, L. Q.; Mao, S. X.; Hudak, N. S.; Liu, X. H.; Subramanian, A.; Fan, H.; Qi. L.; Kushima, A.; Li, J. In situ observation of the electrochemical lithiation of a single SnO_2 nanowire electrode. *Science*, **2010**, 330, 1515-1520.

[13] Hong, Y. J.; Son, M. Y.; Kang, Y. C. One-pot facile synthesis of double-shelled SnO_2 yolk-shell-structured powders by continuous process as anode materials for Li-ion batteries. *Adv. Mater*. **2013**, 25, 2279-2283.

[14] Yang, S.; Yue, W.; Zhu, J.; Ren, Y.; Yang, X. Graphene-Based Mesoporous SnO_2 with Enhanced Electrochemical Performance for Lithium-Ion Batteries. *Adv. Funct. Mater*. **2013**, 23, 3570-3576.

[15] Han, S.; Jang, B.; Kim, T.; Oh, S. M.; Hyeon, T. Simple Synthesis of Hollow Tin Dioxide Microspheres and Their Application to Lithium-Ion Battery Anodes. *Adv. Funct. Mater*. **2005**, 15, 1845-1850.

[16] Lou, X. W.; Wang, Y.; Yuan, C.; Lee, J. Y.; Archer. L. A. Template-Free Synthesis of SnO_2 Hollow Nanostructures with High Lithium Storage Capacity. *Adv. Mater*. **2006**, 18, 2325-2329.

[17] Kim, W.–S.; Hwa, Y.; Jeun, J.–H.; Sohn, H.–J.; Hong, S.–H. Synthesis of SnO_2 nano hollow spheres and their size effects in lithium ion battery anode application. *J. Power Source*, **2013**, 225, 108-112.

[18] Poizot, P.; Laruelle, S.; Grugeon, S.; Dupont, L.; Tarascon, J.–M. Nano-sized transition-metal oxides as negative-electrode materials for lithium-ion batteries. *Nature*, **2000**, 407, 496-499.

[19] Lou, X. W.; Deng, D.; Lee, J. Y.; Feng, J.; Archer, L. A. Self-supported formation of needlelike Co_3O_4 nanotubes and their application as lithium-ion battery electrodes. *Adv. Mater*. **2008**, 20, 258-262.

[20] Laruelle, S.; Grugeon, S.; Poizot, P.; Dollé, Dupont, M.; L.; Tarascon, J. -M. On the origin of the extra electrochemical capacity displayed by MO/Li cells at low potential. *J. Electrochem. Soc*. **2002**, 149 (5), A627-A634.

[21] Kang, Y.–M.; Song, M.–S.; Kim, J.–H.; Kim, H.–S.; Park, M.–S.; Lee, J.–Y.; Liu, H. K.; Dou, S. X. A study on the charge–discharge mechanism of Co_3O_4 as an anode for the Li ion secondary battery. *Electrochimica Acta*, **2005**, 50, 3667-3673.

[22] Qi, Y.; Du, N.; Zhang, H.; Fan, X.; Yang, Y.; Yang, D. CoO/$NiSi_x$ core–shell nanowire arrays as lithium-ion anodes with high rate capabilities. *Nanoscale*, **2012**, 4, 991-996.

[23] Wu, Z.-S.; Ren, W.; Wen, L.; Gao, L.; Zhao, J.; Chen, Z.; Zhou, G.; Li, F.; Cheng, H.-M. Graphene anchored with Co_3O_4 nanoparticles as anode of lithium ion batteries with

enhanced reversible capacity and cyclic performance. *ACS Nano*, **2010**, 4, 3187-3194.

[24] Qi, Y.; Du, N.; Zhang, H.; Wang, J.; Yang, Y.; Yang, D. Nanostructured hybrid cobalt oxide/copper electrodes of lithium-ion batteries with reversible high-rate capabilities. *J. Alloys Compd*. **2012**, 521, 83-89.

[25] Wang, Y.; Xia, H.; Lu, L.; Lin, J. Y. Excellent performance in lithium-ion battery anodes: rational synthesis of $Co(CO_3)_{0.5}(OH)0.11H_2O$ nanobelt array and its conversion into mesoporous and single-crystal Co_3O_4. *Acs Nano*, **2010**, 4, 1425-1432.

[26] Chen, J. S.; Li, C. M.; Zhou, W. W.; Yan, Q. Y.; Archer, L. A.; Lou, X. W. One-pot formation of SnO_2 hollow nanospheres and α-Fe_2O_3@SnO_2 nanorattles with large void space and their lithium storage properties. *Nanoscale*, **2009**, 1, 280-285.

[27] Wang, G.; Gao, X. P.; Shen, P. W. Hydrothermal synthesis of Co_2SnO_4 nanocrystals as anode materials for Li-ion batteries. *J. Power Sources*, **2009**, 192,719-723.

[28] Xing, L. –L.; Zhao, Y. –Y.; Zhao, J.; Nie, Y. –X.; Deng, P.; Wang, Q.; Xue, X. –Y. Facile synthesis and lithium storage performance of SnO_2–Co_3O_4 core–shell nanoneedle arrays on copper foil. *J. Alloys Compd.*, **2014**, 586, 28-33.

[29] Qi, Y.; Zhang, H.; Du, N.; Zhai, C.; Yang, D. Synthesis of Co_3O_4@SnO_2@C core-shell nanorods with superior reversible lithium-ion storage. *RSC Adv.*, **2012**, 2, 9511-9516.

[30] Stöber, W.; Fink, A.; Bohn, E. Controlled growth of monodisperse silica spheres in the micron size range. *J. Colloid Interface Sci.* **1968**, 26, 62-69.

[31] Lou, X. W.; Yuan, C.; Archer, L. A. Shell-by-shell synthesis of tin oxide hollow colloids with nanoarchitectured walls: cavity size tuning and functionalization. *Small*, **2007**, 3, 261-265.

[32] Plank, N. O. V.; Snaith, H. J.; Ducati, C.; Bendall, J. S.; Schmidt-Mende, L.; Welland, M. E. A simple low temperature synthesis route for ZnO–MgO core–shell nanowires. *Nanotechnology*, **2008**, 19, 465603.

[33] Qi, G.; Liu, Y.; Jiao, W.; Zhang, L. Template synthesis of β-$Ni(OH)_2$ hollow microspheres through a hydrothermal process. *Micro & Nano Letters*, **2010**, 5, 278-281.

[34] Qiu, Y.; Yu, J. Synthesis of titanium dioxide nanotubes from electrospun fiber templates. *Solid State Commun.* **2008**, 148, 556-558.

[35] Yim, S. D.; Kim, S. J.; Baik, J. H.; Nam, I.−S.; Mok, Y. S.; Lee, J.–H.; Cho, B. K.; Oh, S. H. Decomposition of urea into NH_3 for the SCR process. *Ind. Eng. Chem. Res*. **2004**, 43, 4856-4863.

[36] Ye, Q.–L.; Yoshikawa, H.; Awaga, K. Magnetic and optical properties of submicron-size hollow spheres. *Materials*, **2010**, 3, 1244-1268.

[37] Liu, Z.; Ma, R.; Osada, M.; Takada, K.; Sasaki, T. Selective and Controlled Synthesis of α- and β-Cobalt Hydroxides in Highly Developed Hexagonal Platelets. *J. Am. Chem. Soc.* **2005**, 127, 13869–13874.

[38] Carson, G. A.; Nassir, M. H.; Langell, M. A. Epitaxial growth of Co_3O_4 on CoO(100). *J. Vac. Sci. Technol. A*, **1996**, 14, 1637-1642.

[39] Burriel, M.; Garcia, G.; Santiso, J.; Abrutis, A.; Saltyte, Z.; Figueras, A. Growth kinetics, composition, and morphology of Co_3O_4 thin films prepared by pulsed liquid-injection MOCVD. *Chem. Vapor Deposition*, 2005, 11, 106-111.

[40] Kim, D. H.; Kwon, J.–H.; Kim, M.; Hong, S.–H. Structural characteristics of epitaxial SnO_2 films deposited on a- and m-cut sapphire by ALD. *J. Crystal Growth*, **2011**, 322, 33-37.

[41] Lian, P.; Zhu, X.; Liang, S.; Li, Z.; Yang, W.; Wang, H. High reversible capacity of SnO_2/graphene nanocomposite as an anode material for lithium-ion batteries. *Electrochim. Acta*, **2011**, 56, 4532-4539.

[42] Lou, X. W.; Chen, J. S.; Chen, P.; L. Archer, A. One-pot synthesis of carbon-coated SnO_2 nanocolloids with improved reversible lithium storage properties. *Chem. Mater.* **2009**, 21, 2868-2874.

[43] Hwa, Y.; Kim, W.–S.; Yu, B.–C.; Kim, H.; Hong, S.–H.; Sohn, H.–J. Reversible storage of Li-ion in nano-Si/SnO_2 core–shell nanostructured electrode. *J. Mater. Chem. A*, **2013**, 1, 3733-3738.

[44] Kilibarda, G.; Szabó, D.V.; Schlabach, S.; Winkler, V.; Bruns, M.; Hanemann, T. Investigation of the degradation of SnO_2 electrodes for use in Li-ion cells. *J. Power Sources*, **2013**, 233, 139-147.

[45] Larcher, D.; Sudant, G.; Leriche, J.–B.; Chabre, Y.; Tarascon, J.–M. The Electrochemical Reduction of Co_3O_4 in a Lithium Cell. *J. Electrochem. Soc*. **2002**, 149 (3), A234-A241.

[46] Aravindan, V. ; Jinesh, K.B.; Prabhakar, R. R.; Kale, V. S.; Madhavi, S., Atomic layer deposited (ALD) SnO_2 anodes with exceptional cycleability for Li-ion batteries. *Nano Energy*, **2013**, 2 (5), 720-725.

Electronic Supplementary Material

$SnO_2@Co_3O_4$ Hollow Nano-spheres for a Li-ion Battery Anode with Extraordinary Performance

Won-Sik Kim, Yoon Hwa, Hong-Chan Kim, Jong-Hyun Choi, Hun-Joon Sohn, and Seong-Hyeon Hong

Won-Sik Kim, Yoon Hwa, Hong-Chan Kim, Jong-Hyun Choi, Hun-Joon Sohn, and Seong-Hyeon Hong
Department of Materials Science and Engineering and Research Institute of Advanced Materials, Seoul National University, Seoul 151-744, Republic of Korea

Supporting information to DOI 10.1007/s12274-****-****-* (automatically inserted by the publisher)

◆ **Comparison of theoretical capacity and measured capacity of $SnO_2@Co_3O_4$ Hollow Nano-spheres electrode.**

: The atomic ratio of Co to Sn determined by EDS was ~0.46, which can be converted to 1:4=Co_3O_4:SnO_2 by weight. The theoretical capacity is, by a rule of mixture,

$$(890\ mA\ g^{-1} \times 1/5)_{Co3O4} + (781\ mA\ g^{-1} \times 4/5)_{SnO2} = 802\ mAh\ g^{-1} \quad (1)$$

At first cycle (discharge capacity = 2208 mAh g^{-1}), there were too many side reactions involved. So we compared the calculated capacity to the second charge capacity (1366 mAh g^{-1}).

When compared with the second charge capacity,

$$1366\ mAh\ g^{-1}\ (\text{second charge capacity}) - 802\ mAh\ g^{-1}\ (\text{theoretical capacity}) = 562\ mAh\ g^{-1} \quad (2)$$

Thus, ~582 mAh g^{-1} was resulted from synergistic effect and reversible growth of gel-like polymeric layer on the surface of Co_3O_4.

If the Li_xSn and Li_2O, generated from SnO_2, were fully reversible to SnO_2, the following capacity can be added.

$$(771\ mAh\ g^{-1}\ (Li_2O\ \text{of}\ SnO_2) \times 4/5) = 616.8\ mAh\ g^{-1} \quad (3)$$

Address correspondence to First Seong-Hyeon Hong, email; shhong@snu.ac.kr

But, our TEM results showed that the partial recombination reaction between Sn and L_2O occurred and formed the SnO.

Thus, the participated theoretical capacity of Li_2O, to form SnO, is,

$$1/2\ \{771\ mAh\ g^{-1}\ (Li_2O\ of\ SnO_2)\}\ x\ 4/5 = 308.4\ mAh\ g^{-1} \quad (4)$$

The difference between measured capacity and theoretical capacity from (2) is 562 mAh g^{-1}.

As a result, the reversible capacity consisted of following components,

$$802\ mAh\ g^{-1}\ (mixture\ rule\ of\ SnO_2\ and\ Co_3O_4) + 308.4\ mAh\ g^{-1}\ (partial\ recombination\ reaction\ to\ SnO)$$
$$+ 255.6\ (SEI\ formation\ or\ additional\ reaction) = 1366\ mAh\ g^{-1}\ (measured\ capacity) \quad (5)$$

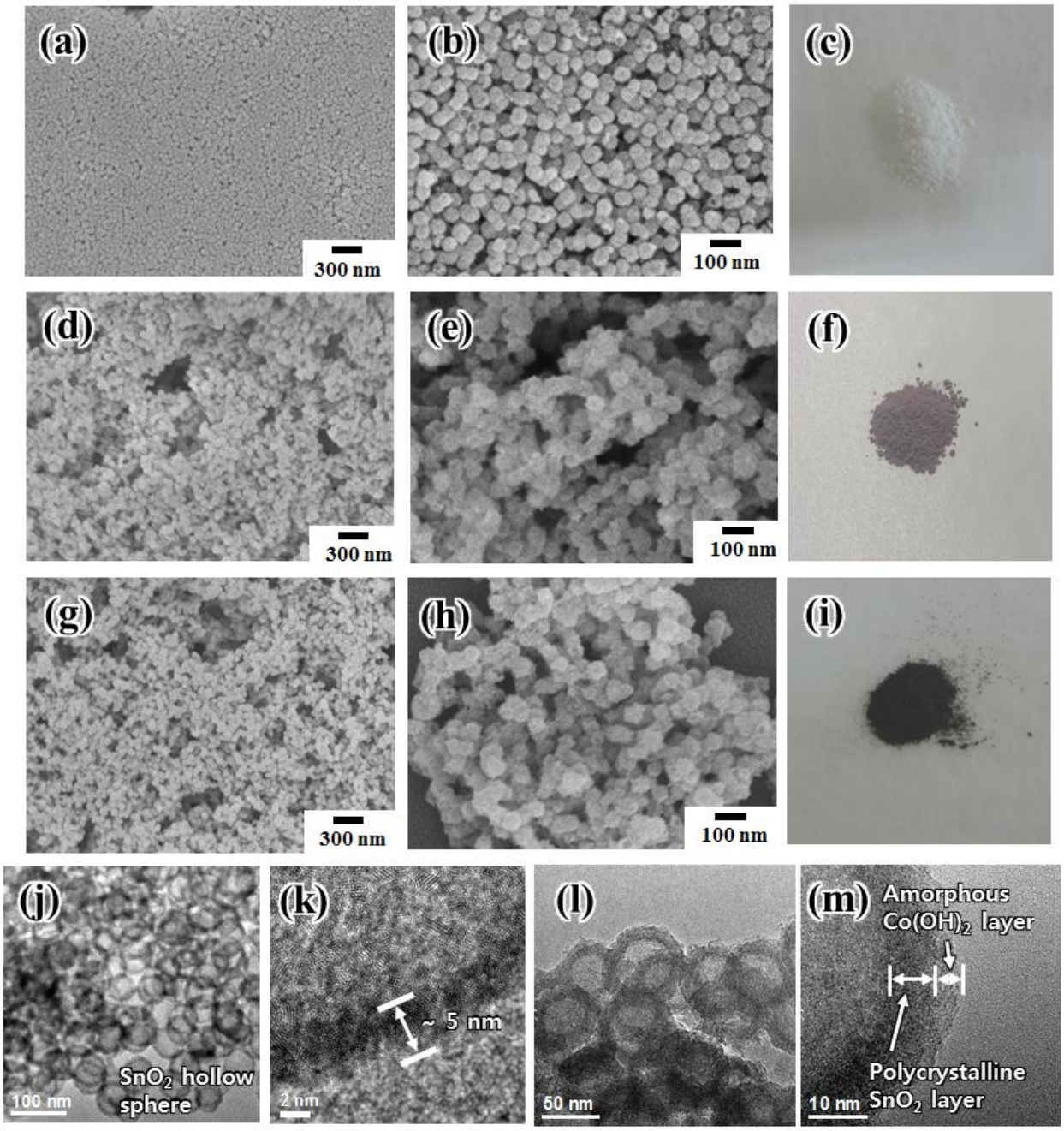

Fig. S-1. SEM and optical camera images; (a-c) SnO_2 hollow sphere, (d-f) as-synthesized SnO_2@$Co(OH)_2$, (g-i) annealed SnO_2@Co_3O_4.. TEM images of (j, k) SnO_2 hollow nano-spheres and (l, m) as-synthesized SnO_2@$Co(OH)_2$.

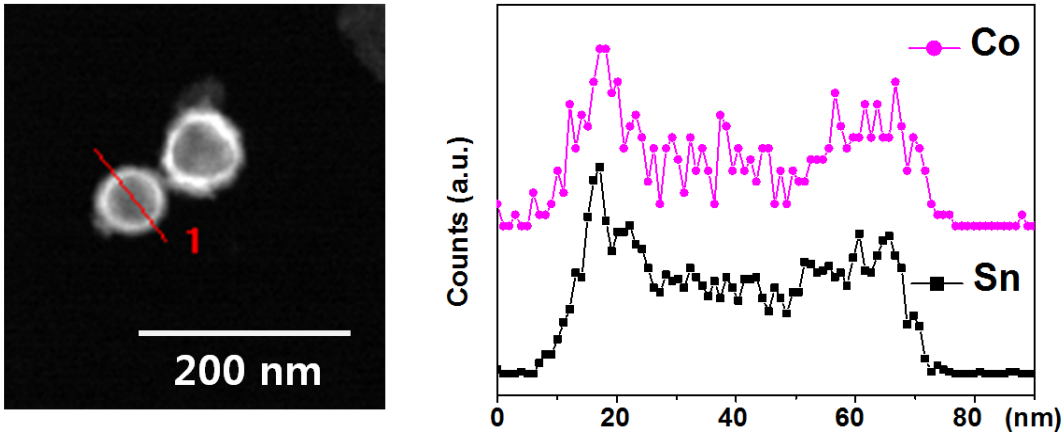

Fig. S-2 Line scan profile of Co and Sn elements in SnO_2@Co_3O_4 hollow nano-sphere.

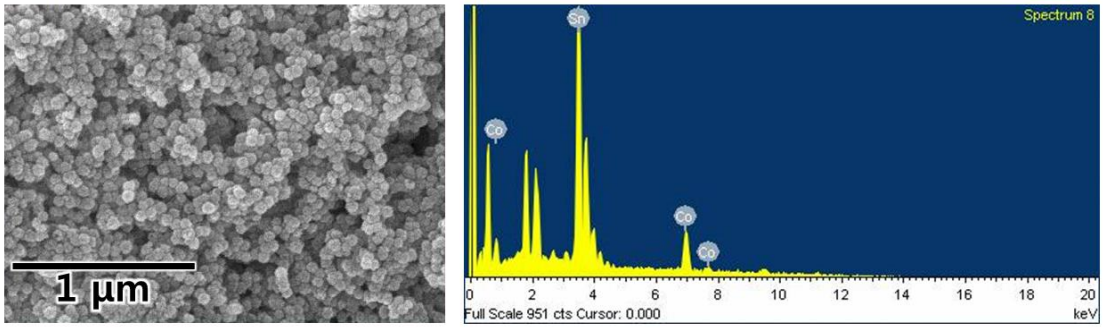

Element	Average weight %	Average Atomic %
Co	18.73	31.68
Sn	81.27	68.32

Fig. S-3 EDS results of SnO_2@Co_3O_4 hollow nano-spheres.

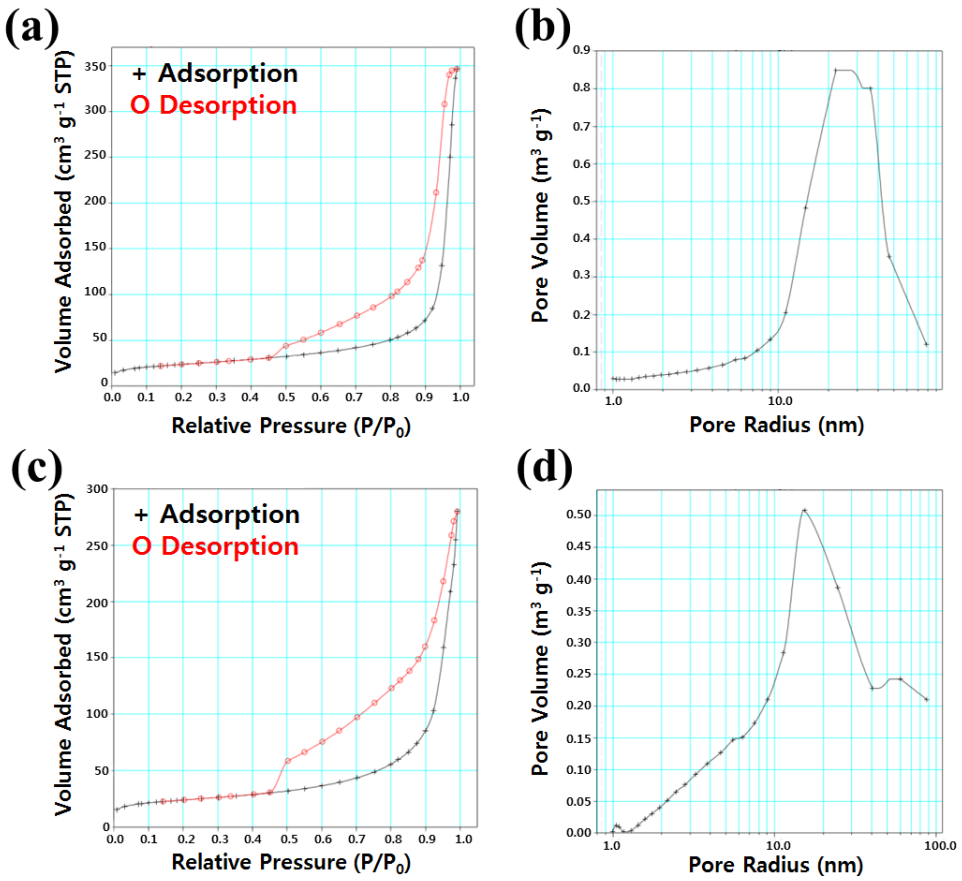

Fig. S-4 (a) and (b) Nitrogen absorption-desorption isotherm and pore size distribution of SnO_2 hollow sphere, (c) and (d) Nitrogen absorption-desorption isotherm and pore size distribution of $SnO_2@Co_3O_4$ hollow sphere. (BET surface area of SnO_2 and $SnO_2@Co_3O_4$ hollow spheres was 84.32 and 84.47 $m^2\ g^{-1}$, respectively. The BJH adsorption average pore radius of SnO_2 and $SnO_2@Co_3O_4$ hollow spheres was 13.90 and 11.88 nm, respectively)

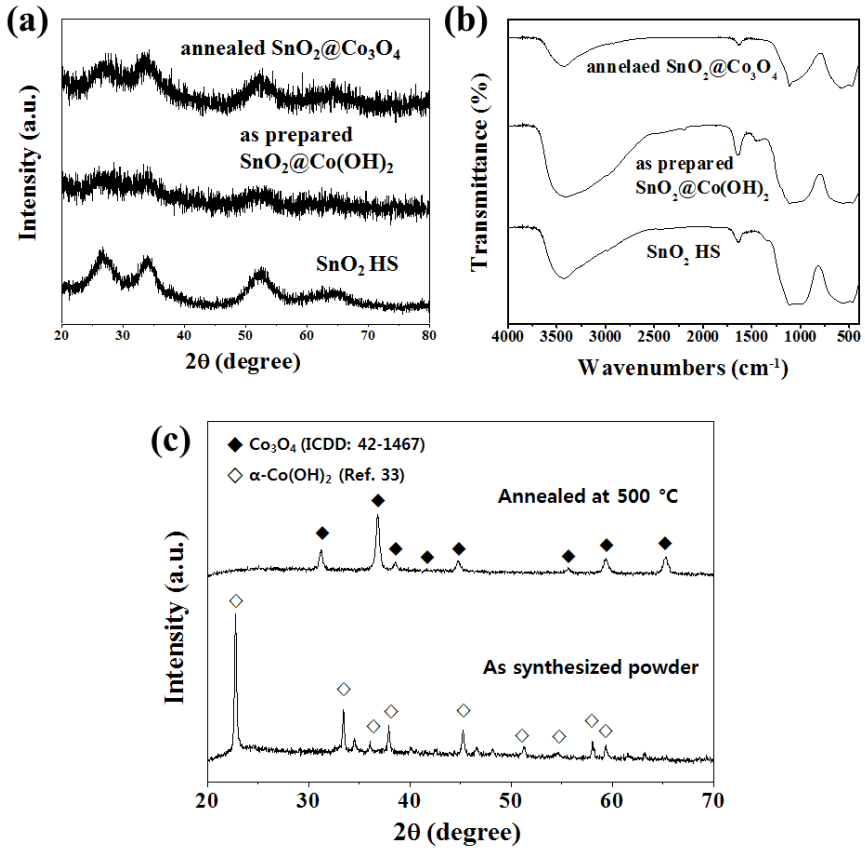

Figure S-5. (a) XRD patterns and (b) FTIR spectra of as-synthesized SnO_2, SnO_2@$Co(OH)_2$, and SnO_2@Co_3O_4, (c) XRD pattern of as synthesized $Co(OH)_2$ and annealed Co_3O_4 powder without SnO_2 core.

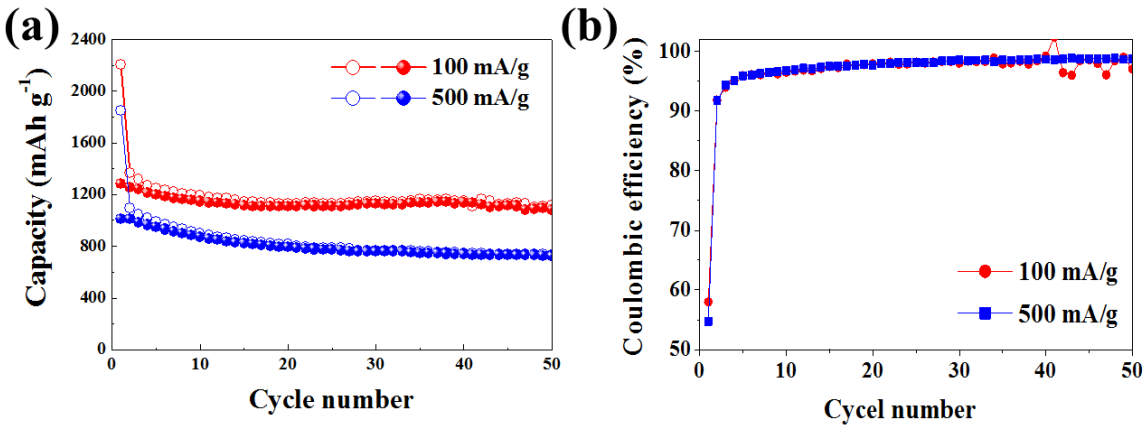

Fig. S-6 (a) Cycling performance of SnO_2@Co_3O_4 hollow spheres at 100 and 500 mA g^{-1}, (b) Columbic efficiency at 100 and 500 mA g^{-1}.

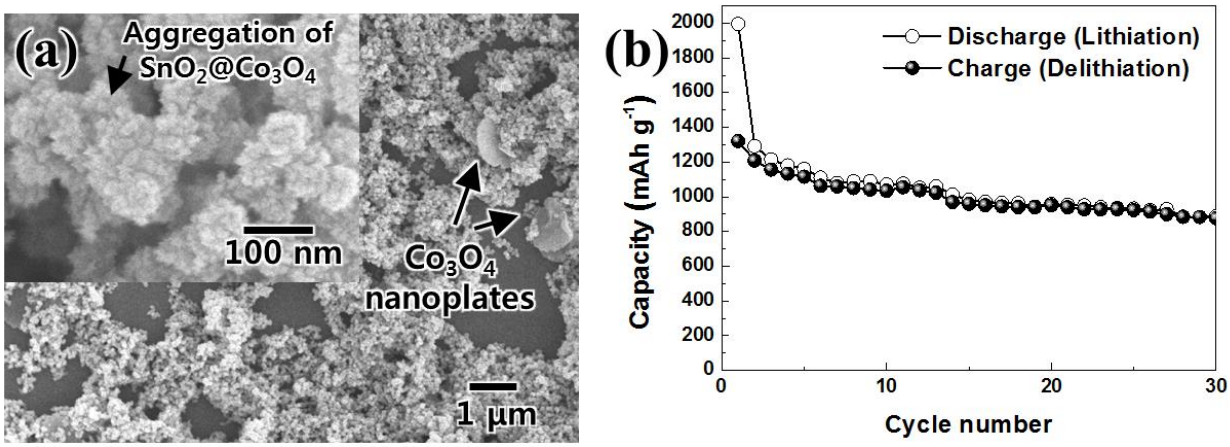

Fig. **S-7** (a) SEM image and (b) cycling performance of SnO_2@Co_3O_4 hollow spheres with a large amount of Co precursor ($Co(NO_3)_2 \cdot 6H_2O$). With increasing the Co precursor, the aggregation of SnO_2@Co_3O_4 was severe and Co_3O_4 nanoplates were formed as a byproduct. And this electrode showed a fast capacity fading at current density of 100 mA g^{-1} (1324 mAh g^{-1} at 1st cycle and 887 mAh g^{-1} at 30 cycles).

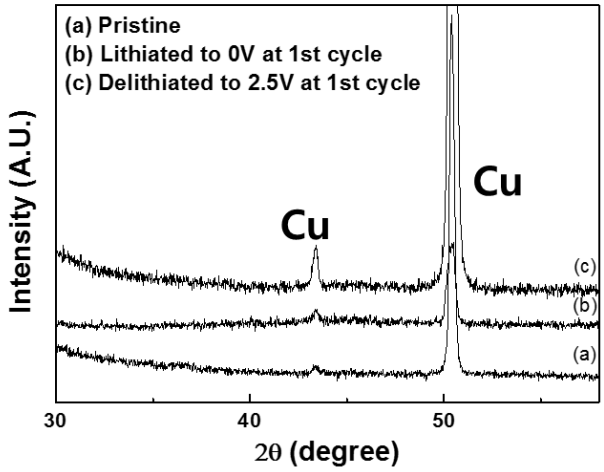

Fig. S-8 Ex-situ XRD analysis. (a) pristine electrode, (b) discharged to 0 V, and (c) charged to 2.5 V.